Gas Permeability of Porous Plasma-Sprayed Coatings

K. Wittmann-Ténèze, N. Caron, and S. Alexandre

For different applications, such as solid oxide fuel cells, there is an interest in understanding the relationship between the microstructure and the gas permeability of plasma-sprayed coatings. Nevertheless, plasma spraying processes allow to elaborate coatings with singular microstructures, depending strongly on the initial material and plasma operating conditions. And so, the evolution of permeability is not directly linked to the porosity. In this work, coatings were manufactured using different initial feedstock and spray parameters to obtain various microporous structures. Measurements of their permeation with the pressure drop method and their open porosity just as the observation of the morphology and the structure by optical microscopy were achieved. The different data show that the evolution of the gas permeability with the open porosity follows the Kozeny-Carman equation. This result correlated with the microstructural observation highlights the relationship between the permeability and the physical properties of porous plasma-sprayed layers.

1. Introduction

Porous materials attracted much attention due to their wide use in many modern applications such as fuel cell or biological materials. They are very often characterized in terms of porosity but not in terms of gas permeability. Though, the permeability of electrode layers in the solid oxide fuel cell (SOFC) field, for example, is an essential quality for their performance at the operating conditions of the SOFC system: flow resistance in the material determines the power losses, particularly at high power outputs and high gas exchange rate (Ref 1). Nevertheless, little information about gas permeability of porous ceramics exists in the literature. Most of studies deal with water permeability through ceramic membranes for environmental, petrochemical, and food industries (Ref 2-4) or

with gas permeability of dense ceramic layers for SOFC or thermal barrier coatings applications (Ref 5-10). Those works underline that permeability is dependent of the microstructural properties of a porous medium. It can be estimated by the Kozeny-Carman (KC) equation, a classical semiempirical relation applied in various fields such as chemical engineering, medicine, biochemical, and electrochemical engineering (Ref 11).

The microstructure of thermally sprayed coatings is very peculiar, lamellar, and anisotropic, depending strongly on the initial material and plasma conditions. During the manufacturing step, a natural porosity is created. The resulting pores can be arranged in three categories (Ref 12-14): globular pores, interlamellar pores, and interlamellar cracks (in the case of ceramics). To this natural porosity, it is possible to add an artificial one increasing the porosity level by using an agent favoring the generation of globular pores. The characterization of such microstructure is more pertinent using a permeability factor rather than a porosity level. Very few studies were done on this topic and most of them were achieved in the SOFC field (Ref 1, 15).

The present work aims at establishing the relationship between gas permeability and microstructure of porous plasma-sprayed coatings, which may be helpful to underline the optimized coating microstructure for better permeation performance.

2. Experiments

2.1 Starting Feedstock Material

Commercial ceramic and metallic powders were used as feedstock material. Ceram 1 and Ceram 2 are both a mixture of two ceramic oxides having the same composition. Ceram 2 and Metal have the same particle size and

K. Wittmann-Ténèze, N. Caron, and **S. Alexandre**, Plasma Spraying Laboratory, CEA Le Ripault, BP 16, 37260 Monts, France. Contact e-mails: karine.wittmann-teneze@cea.fr; nadege.caron@cea.fr and samuel.alexandre@cea.fr.
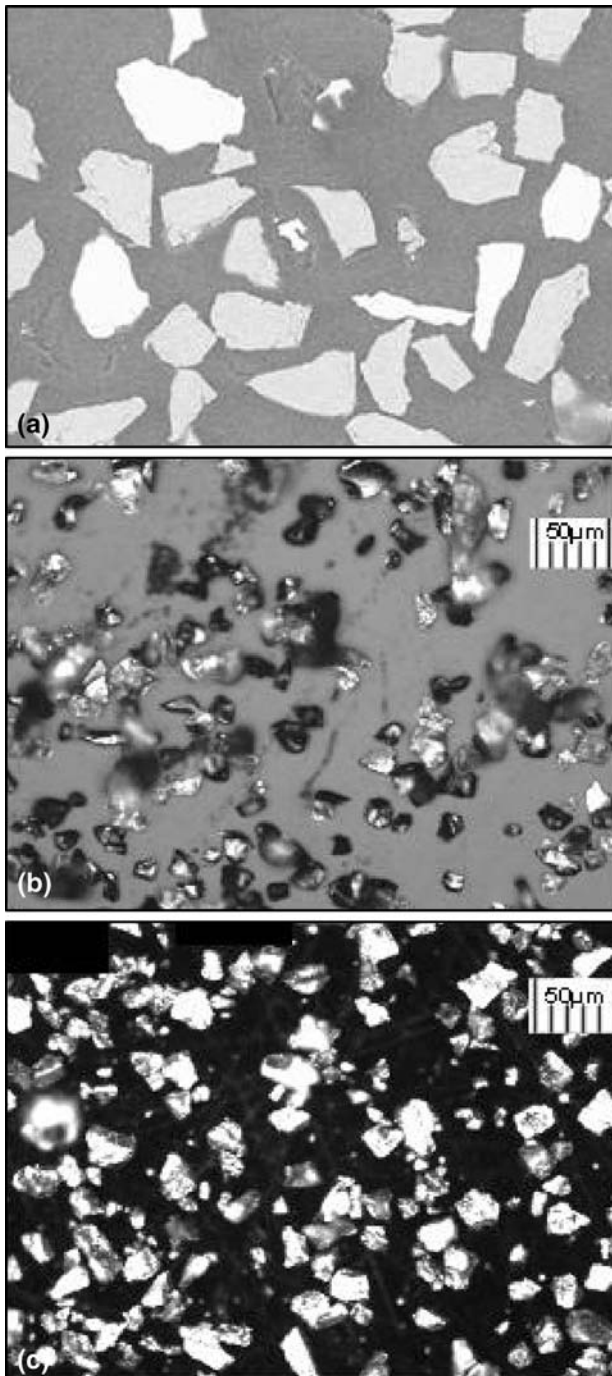
Fig. 1 Optical images of the fused and crushed powders: (a) Ceram 1, (b) Ceram 2, and (c) Metal

Table 1 Feedstock particle sizes

Powder	Ceram 1	Ceram 2	Metal
Particle size, μm			
d_{10}	40	15	15
d_{50}	49	24	25
d_{90}	90	40	45

2.2 Spray Parameters

Plasma spraying was performed with a F100-Connex torch (Sulzer-Metco, Wohlen, Switzerland) under inert atmosphere (argon at atmospheric pressure) to avoid metallic particles oxidation. Table 2 summarizes the five plasma conditions used; standoff distance, injector diameter, powder feed rate, gun traverse speed, and substrate temperature were maintained constant for all the spraying conditions.

The condition C1 was used for Metal powder, C2 for Ceram 2, and the three others for Ceram 1. Conditions C1 to C3 were adapted to the different powder characteristics; each of them resulting from a parametric study that aimed at identifying operating parameters permitting to form a cohesive coating with a high deposition rate.

For the powder Ceram 1, two other conditions were used: C4 having a higher plasma jet velocity than C3 and C5 generating a higher enthalpy plasma by adjusting appropriately the operating parameters.

The centerline velocity of the plasma jet at the nozzle exit, V_{plasma}, was predicted by the formula (Ref 16):

$$V_{plasma} \approx R_{th} \cdot \frac{U \cdot I}{p \cdot S_{anode}} \cdot \frac{\gamma - 1}{\gamma} \quad \text{(Eq 1)}$$

where p is the atmospheric pressure, S_{anode} is the cross section area of the channel, R_{th} is the thermal efficiency of the torch, V is the arc voltage, I is the arc current, and γ is the isentropic coefficient.

The calculated values for conditions C1 to C5 are given in Table 3.

Aluminum substrates, 30 mm in diameter and 2 mm in thickness, were prepared by grit blasting and degreasing before spraying. To obtain, in a second time, self-supported coatings for permeation measurements, the substrates were covered with a soluble layer that was solubilized in a second time. During coating manufacturing, the substrate temperature was maintained at a temperature lower than 100 °C by means of liquid argon cooling.

2.3 Porosity Measurements

The open porosity of the self-supported coatings was measured using the hydrostatic pressure method based on the Archimedes principle. The sample is carefully dried in a furnace and its weight, w_d, is measured. It is then impregnated with water under soft vacuum. It is placed on a support in water. The immerged weight, w_i, is measured. At last, the sample is withdrawn from the water and is delicately wiped to measure the humid weight, w_h. The open porosity, ε, of the sample is given by Eq. 2:

morphology (Fig. 1a, c) whereas Ceram 1 consists of higher diameter particles (Fig. 1b). The different particle size distributions given by the supplier are presented in Table 1.

A solid agent favoring the generation of pores was co-sprayed to generate the open porosity of coatings. Thus, by increasing its proportion, open porosity up to 55% was achieved in this work.

Table 2 Plasma spraying conditions

Conditions: Powder:	C1 Metal	C2 Ceram 2	C3 Ceram 1	C4 Ceram 1	C5 Ceram 1
Injector diameter, mm	1.8	1.8	1.8	1.8	1.8
Anode internal diameter, mm	6	6	6	6	6
Ar, NL/min	20	24	25	34	14
He, NL/min	30	16	0	0	24
H₂, NL/min	0	3	5	6	4
Arc current intensity, A	450	450	450	550	500
Plasma flow mass enthalpy, kJ/g	10	18	19	18	33
Spray distance, mm	100	100	100	100	100

Table 3 Centerline velocities of the different plasma jets at the nozzle exit

	C1	C2	C3	C4	C5
V_{plasma}, m/s	500	790	800	1000	940

$$\varepsilon \, (\%) = \frac{w_h - w_d}{w_h - w_i} \times 100 \tag{Eq 2}$$

The determination of the open porosity is made three times on the same coating and the given ε in this work is the average of those three values.

This method to determine the porosity, even if the quantitative value remains hard to measure with accuracy, avoids the polishing step, necessary in the case of porosity measurement by image analysis, which is very often a source of mistakes. Moreover, for this work, it is the open porosity which is the more pertinent value (instead of the total or closed porosity) because it participates in the fluid permeability.

2.4 Gas Permeability Measurements

As-sprayed coating permeability was assessed by the pressure drop method. Several forced air flow rates are applied on one face of the measured porous coating, the other face being at atmospheric pressure. The resulting pressure drop is measured for each air flow rate. After checking the linear evolution of the pressure drop with the gas flow rate, the permeability can be measured with the Darcy's law (Ref [17]):

$$Q = k \cdot \frac{A \cdot \Delta P}{\eta \cdot e} \tag{Eq 3}$$

where Q is the air mass flow rate (m³/s) through a cross-sectional area A (m²), η is the air cinematic viscosity (Pa.s), ΔP is the pressure drop (Pa) over a coating thickness e (m), and k is the permeability of the material (m²).

3. Permeability Evolution of Coatings

In this work, it is on interest to correlate the permeability of a plasma-sprayed coating to its microstructure

(specific area, particle and pore geometry, particle nature, etc.). A relation proposed by Kozeny and later modified by Carman (Ref [18], [19]) has been used to describe a laminar flow through a porous medium. This semiempirical KC equation is the most used permeability-porosity relation:

$$k = \frac{1}{k_c \cdot S_v^2} \cdot \frac{\varepsilon^3}{(1-\varepsilon)^2} \tag{Eq 4}$$

where ε is the porosity level (between 0 and 1) of the medium, S_v is the specific surface area per volume (m^{-1}) of this medium, k_c is the Kozeny factor which depends itself on porosity, microstructures of pores, and capillaries (Ref [11]).

The Kozeny factor is defined by:

$$k_c = 2\gamma \left(\frac{L_p}{e} \right)^2 \tag{Eq 5}$$

where γ is a constant defined by the shape of the cross section of the flow channel, L_p is the real length of the flow channel (m), and e is the thickness of the coating (m). The ratio (L_p/e) is also called the tortuosity, a nonindependent factor, varying with many parameters, such as porosity or geometry of porous media (Ref [20]). Its value has a theoretical minimum of 1 and a reasonable maximum of 1.4.

Increasing the coating porosity level is the first reflex that favors permeability. Nevertheless, a too high porosity (particularly for ceramics) impedes the mechanical performances of the porous material. So, it is on interest to understand other parameters which can influence the coating permeability (pores and particles geometry, particles size and spreading, etc.). The KC equation can be a pertinent tool to correlate plasma coating microstructures (and so, spray parameters) to its gas permeability.

To be easily interpreted, the KC equation for the same initial powder can be expressed as follows:

$$k = A_i \cdot \frac{\varepsilon^3}{(1-\varepsilon)^2} \tag{Eq 6}$$

where $A_i = e^2 / (2\gamma \cdot L_p^2 \cdot S_v^2)$ is a proportional coefficient for the powder i, depending on the sprayed material microstructure.

3.1 Correlation Between Porosity and Permeability

Coatings with different porosity levels adjusted by varying the porous agent proportion were realized with the three initial powders to characterize their permeability.

Figure 2 shows the evolution of the air permeability, measured and calculated with the KC equation, of coatings with their porosity. Here, Ceram 1 was sprayed with condition C3. The value of A_i is estimated by correlating the KC equation (following Eq. 6) to the experimental data.

From Fig. 2, several observations were made:

- The KC relation can be applied on thermal-sprayed porous coatings (with a porosity rate between 20%
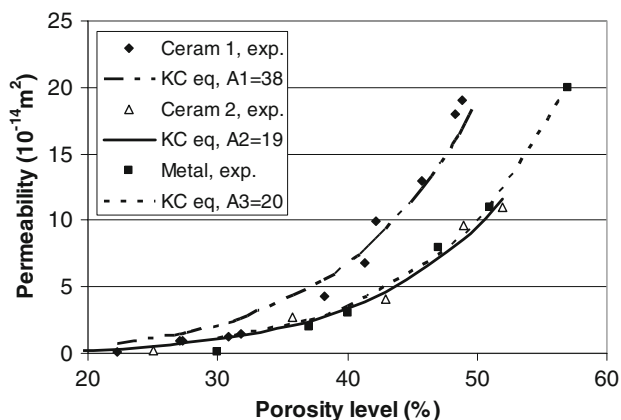
Fig. 2 Influence of the open porosity on the permeability of plasma-sprayed porous coatings elaborated with three different initial powders

and 55%) for the three initial powders, regardless of their nature and size, because of the well-fitting of the experimental results with the theoretical curb.

- The same evolution of the permeability with the porosity is observed for coatings elaborated with Ceram 2 and Metal, having the same initial particle size distribution.

- The higher the powder particle average size, the higher is the value of A_i: Ceram 1 having a d_{50} of 49 μm, A_i is equal to 38 and Ceram 2 and Metal having a d_{50} of 24 and 25 μm, A_i values come close to 20 and 19, respectively.

The relation between porosity and permeability seems to be more influenced by the initial particle size than their nature in the evaluated range of porosities (between 20% and 55%).

The higher A_i, the more advantageous is the coating microstructure to favor high permeability values. Microstructure of coatings elaborated with the three different powders but having a same porosity rate (about 30%) were observed in cross section by optical microscopy (Fig. 3).

In Fig. 3, the black zones correspond to the porosity and the gray zones to ceramic or metallic-sprayed particles.

The most significant result is that particles are more well spread in the case of coatings elaborated with the finer initial particles (Fig. 3b, c). It leads to a higher value of tortuosity (and so a lower value of A_i) and the gas path being longer.

On the contrary, the Ceram 1 coating (Fig. 3a) is constituted of not very well spread splats and almost circular-shaped particles. In that case, the tortuosity is lower (and so the value of A_i is higher) and the gas path through the layer is shorter.

To confirm these first partial conclusions, coatings were sprayed with different plasma jet enthalpies and velocities which directly influence the particle spreading by affecting their viscosity and momentum upon impact.
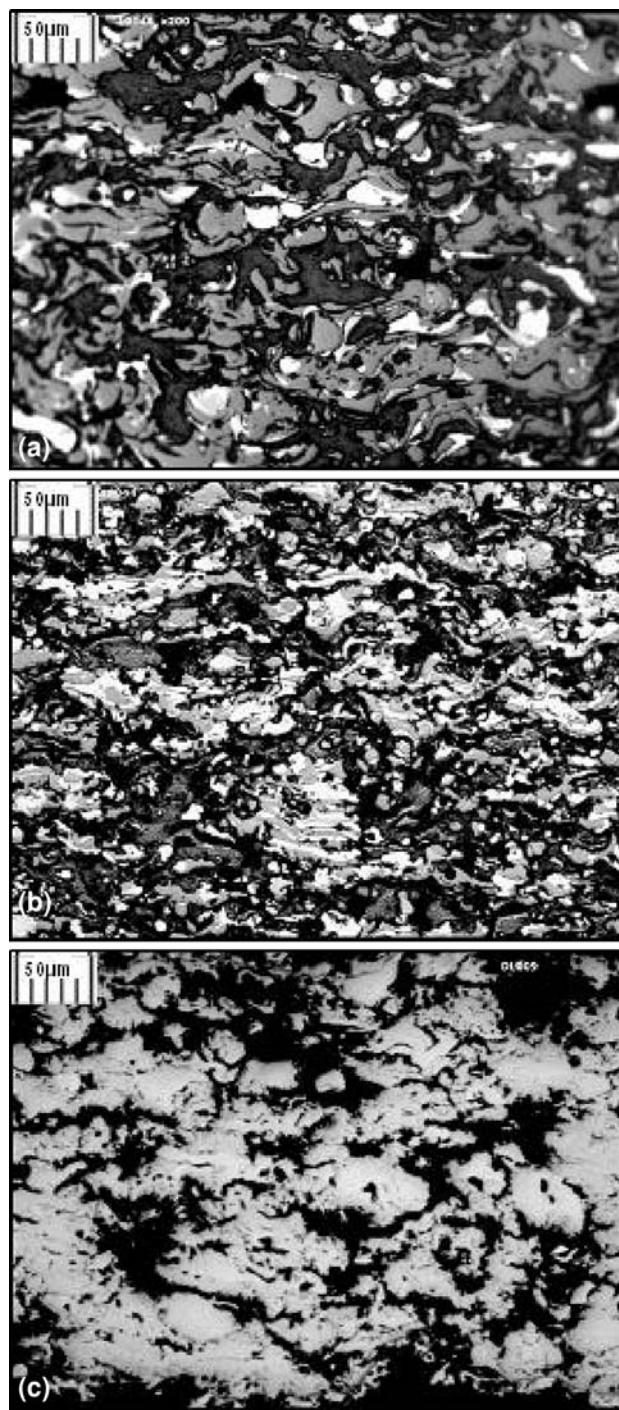

Fig. 3 Optical microscopy of polished cross-section microstructure of coatings elaborated with the three different powders: (a) Ceram 1, (b) Ceram 2, and (c) Metal following conditions C3, C2, and C1, respectively

3.2 Influence of Plasma Jet Properties on Permeability

The influence of the average plasma mass enthalpy, h, on the permeability was studied with the higher average particle size powder (Ceram 1). This powder was sprayed
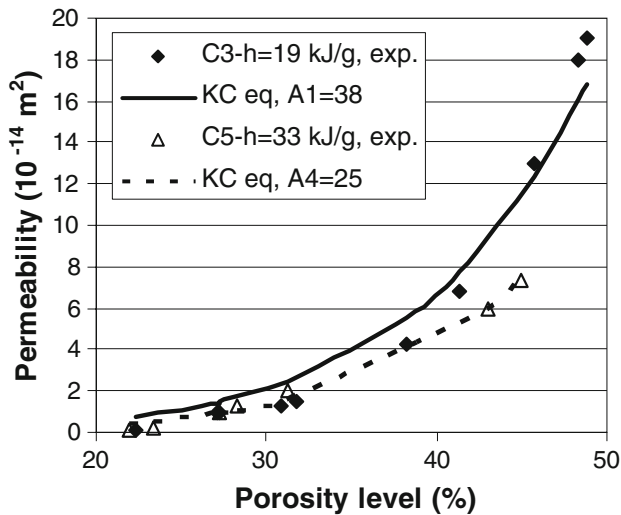
Fig. 4 Influence of the open porosity on the permeability of plasma-sprayed porous coatings elaborated with the same Ceram 1 powder and two plasma jets having different enthalpy values

with C3 ($h = 19$ kJ/g) and C5 ($h = 33$ kJ/g) conditions (Table 2).

Figure 4 shows that A_i is lowered when the mass enthalpy is increased. In that example, a variation of the mass enthalpy of 40% induces a variation of the permeability of 35%. This can be explained quite easily: a higher plasma enthalpy is favorable to a good particle treatment in flight in the plasma jet conducting to well-spread particles. It results in a quite high tortuosity increasing the gas path through the coating and so a lower value of A_i and so a smaller permeability.

The influence of plasma jet velocity on the permeability was also studied with Ceram 1. The plasma conditions that were used are C3 and C4. As mentioned in Table 3, the centerline velocity of the plasma jet at the nozzle exit is 800 m/s for C3 and 1000 m/s for C4. Figure 5 shows that A_i is higher when plasma velocity is lowered. A possible explanation is that particles accelerated more given a more tortuous microstructure when they impact on the substrate.

Though, this result can be explained by comparing Fig. 6 with Fig. 3(b): the microstructure of the coating elaborated with condition C4 is composed of shredded particles. It results in a higher tortuosity and so a lower value of A_i (and so a lower permeability).

4. Conclusion

To increase the gas permeability of a plasma spray coating, the first possibility is to increase its porosity level, for example, by adding a porous agent. Nevertheless, a too high porosity, particularly for ceramics, can affect its mechanical resistance.

The present work, supported by the KC relation, showed that microstructure can also be modified by varying the thermal spray parameters to control the
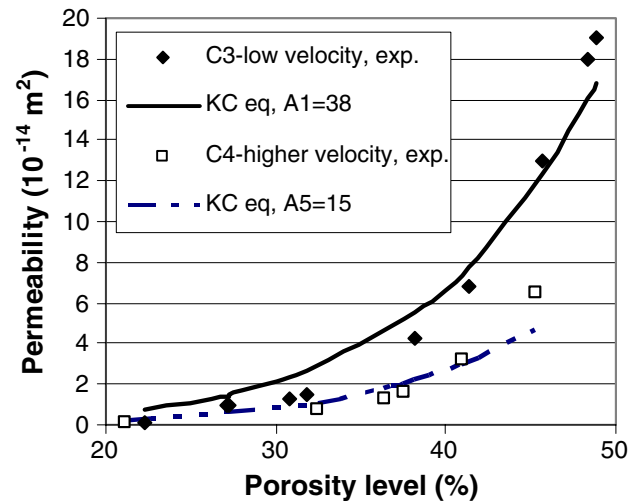

Fig. 5 Influence of the open porosity on the permeability of plasma-sprayed porous coatings elaborated with the same Ceram 1 powder and two plasma jets having different velocities (C3—lowest velocity and C4—highest velocity)
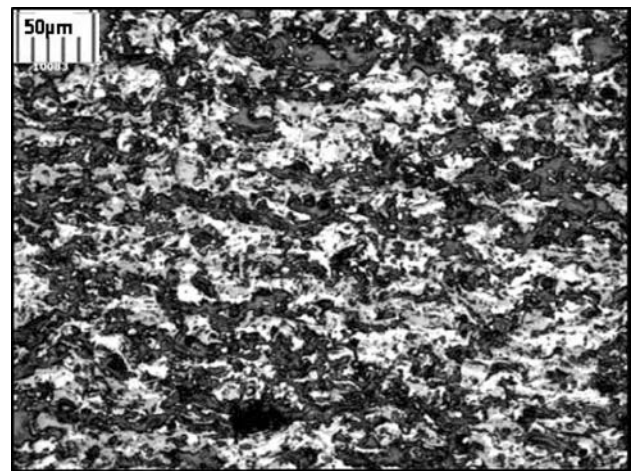

Fig. 6 Optical microscopy of polished cross-section microstructure of a coating elaborated with powder Ceram 1 and condition C4

permeability. A well-adapted coating seems to be composed of particles that are weakly spread to a low tortuous structure. Following this study, the main spraying parameters that can increase the permeability of a porous coating are a high initial particle size, a low plasma mass enthalpy, and a low plasma jet velocity.
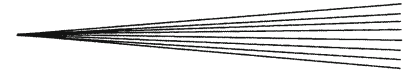
References

1. H. Weckmann, A. Syed, Z. Ilhan, and J. Arnold, Development of Porous Anode Layers for Solid Oxide Fuel Cell by Plasma Spraying, *Proceedings of the 2006 International Thermal Spray Conference*, R. Marple, M. Hyland, Y. Lau, R. Lima, and J. Voyer, Eds., May 15-18, 2006 (Seattle, WA), ASM International, 2006

2. W. Li, W. Xing, and N. Xu, Modeling of Relationship Between Water Permeability and Microstructure Parameters of Ceramic Membranes, *Destination*, 2006, **192**, p 340-345

3. I.H. Huisman, B. Dutre, K.M. Persson, and G. Tragardh, Water Permeability in Ultrafiltration and Microfiltration: Viscous and Electroviscous Effects, *Destination*, 1997, **113**, p 95-103

4. K.M. Persson, V. Gekas, and G. Tragardh, Study of Membrane Compaction and Its Influence on Ultrafiltration Water Permeability, *J. Membr. Sci.*, 1995, **100**, p 155-162

5. C.J. Li, C.X. Li, and X.J. Ning, Performance of YSZ Electrolyte Layer Deposited by Atmospheric Plasma Spraying for Cermet-Supported Tubular SOFC, *Vacuum*, 2006, **73**, p 699-703

6. C. Zhang, C.J. Li, H. Liao, M.P. Planche, C.X. Li, and C. Coddet, Effect of In-Flight Particle Velocity on the Performance of Plasma-Sprayed YSZ Electrolyte Coating for Solid Oxide Fuel Cells, *Surf. Coat. Technol.*, 2008, **202**, p 2654-2660

7. A.C. Fox and T.W. Clyne, Oxygen Transport by Gas Permeation Through the Zirconia Layer in Plasma Sprayed Thermal Barrier Coatings, *Surf. Coat. Technol.*, 2004, **184**, p 311-321

8. K. Marumoto, S. Aya, and Y. Matsui, Characterization of Solid Oxide Fuel Cell Components by Gas Permeability Measurement, *JSME Int. J., Series 2*, 1992, **35**, p 293-299

9. J.R. Mawdsley, Y.J. Su, K.T. Faber, and T.F. Bernecki, Optimization of Small-Particle Plasma-Sprayed Alumina Coatings Using Design Experiments, *Mater. Sci. Eng.*, 2001, **A308**, p 189-199

10. S.J. Oh, J. Joseph, T. Otagawa, and M. Madou, Multilayer Ionic Devices Fabricated by the Plasma Spray Method, *Solid State Ionics*, 1992, **53**(6), p 90-94

11. P. Xu and B. Yu, Developing a New Form of Permeability and Kozeny-Carman Constant for Homogeneous Porous Media by Means of Fractal Geometry, *Adv. Water Resour.*, 2008, **31**, p 74-81

12. C.J. Li, Y. He, and A. Ohmori, Characterization of Structure of Thermally Sprayed Coating, *Proceedings of the 15th International Thermal Spray Conference*, C. Coddet, Ed., May 25-29, 1998 (Nice, France), ASM International, 1998, p 717-722

13. A.J. Allen, J. Ilavsky, G.G. Long, J.S. Wallace, C.C. Berndt, and H. Herman, Microstructural Characterization of Yttria Stabilized Zirconia Plasma-Sprayed Deposits Using Multiple Small-Angle Neutron Scattering, *Acta Mater.*, 2001, **49**, p 1661-1675

14. G. Antou, G. Montavon, F. Hlawska, A. Cornet, and C. Coddet, Exploring Thermal Spray Grey Alumina Coating Pore Network Architecture by Combining Stereological Protocols and Impedance Electrochemical Spectroscopy, *Proceedings of the 2006 International Thermal Spray Conference*, B.R. Marple, M.M. Hyland, et al., Ed. (Seattle, WA), ASM International, 2006, CD ROM

15. Y. Kaga, Y. Ohno, K. Tsukamoto, and F. Uchiyama, Relationships Between the Gas Permeabilities and the Microstructures of Plasma Sprayed Oxide Layers, *Solid State Ionics*, 1990, **40-41**, p 1000-1002

16. J. Fazilleau, "Contribution to the Understanding of the Phenomena Implied in the Achievement of Finely Structured Oxides Coatings by Suspension Plasma Spraying." Ph.D. Thesis, University of Limoges, France, 2003 (in French)

17. S. Zhu, R.H. Pelton, and K. Collver, Mechanistic Modelling of Fluid Permeation Through Compressible Fiber Beds, *Chem. Eng. Sci.*, 1995, **50**(22), p 3557-3572

18. P.C. Carman, Fluid Flow Through Granular Beds, *Trans. Inst. Chem. Eng.*, 1937, **15**, p 150-167

19. P.C. Carman, Permeability of Saturated Sands, Soils and Clays, *J. Agric. Sci.*, 1938, **29**, p 263-273

20. J.H. Azar, A. Javaherian, M.R. Pishvaie, and M. Nabi-Bidhendi, An Approach to Defining Tortuosity and Cementation Factor in Carbonate Reservoir Rocks, *J. Petrol. Sci. Eng.*, 2008, **60**, p 125-131